Journal of Applied Electrochemistry **34**: 545–550, 2004.

Protective properties of an inhibitor layer formed on copper in neutral chloride solution

H. OTMAČIĆ[1], J. TELEGDI[2], K. PAPP[2] and E. STUPNIŠEK-LISAC[1,*]
[1]*Faculty of Chemical Engineering and Technology, University of Zagreb, Savska c. 16, 10000 Zagreb, Croatia*
[2]*Chemical Research Center, Institute of Chemistry, H-1025 Budapest, Hungary*
*(*author for correspondence, fax: +385 1 4597 260, e-mail: elisac@fkit.hr)*

Received 28 July 2003; accepted in revised form 1 November 2003

Key words: AFM, copper corrosion, corrosion inhibitor, cyclic voltammetry, imidazole, SEM/EDX

Abstract

The aim of this work was to investigate the efficiency of 1-phenyl-4-methylimidazole for corrosion inhibition of copper in 3% NaCl solution. The formation of a thick layer on the copper surface was observed in the presence of this compound. The protective properties of this layer were characterized by means of cyclic voltammetry and through AFM and SEM/EDX measurements. Voltammetric measurements were performed in stirred and quiescent solutions as well as at different immersion times. Voltammetric measurements showed that the protective properties of the layer were enhanced by stirring and with an increase in immersion time. The time dependence of the protective layer formation was characterized by AFM measurements. From SEM/EDX measurements it was concluded that this protective layer has a complex structure consisting of the inhibitor and corrosion products.

1. Introduction

One of the most important methods for the corrosion protection of copper is the use of organic inhibitors. Various imidazole derivatives have proven to be effective as copper corrosion inhibitors in many corrosive media [1–11]. Substitution by different functional groups can improve the efficiency of imidazole. Our previous investigations have shown that imidazoles containing phenyl ring have high inhibiting efficiency, much higher than the basic imidazole molecule [8–11]. This effect is due to the electrondonating effect of the phenyl ring, which increases electron density of the imidazole ring.

Electrochemical and gravimetric measurements described previously [11] have shown that 1-phenyl-4-methylimidazole (PhIm) significantly reduces the copper corrosion rate in 3% NaCl solution. In the presence of this inhibitor, a thick inhibitor layer forms and its polarization resistance is 20 times higher than that of an unprotected copper surface. The aim of this work is to study the inhibiting mechanisms and protective properties of this inhibitor layer.

2. Experimental details

2.1. *Materials*

The working electrode and disc for AFM and SEM measurements were of pure copper (99.98% purity). The 1-phenyl-4-methylimidazole was synthesized especially for this research. The 3% NaCl solution was prepared using analytical grade NaCl and bidistilled water. 1-phenyl-4-methylimidazole was used in 5 mmol dm^{-3} concentration which was found to be optimal in our previous investigations [11].

2.2. *Methods*

Cyclic voltammetric measurements were conducted using a PAR 263A potentiostat/galvanostat. A conventional three-electrode cell (~100 cm^3 volume) was used. A saturated calomel electrode (SCE) with a Luggin capillary was the reference and a Pt plate was the counter electrode. All potentials are reported vs SCE. The working electrode, insulated with polytetrafluorethylene so that the exposed area was 0.71 cm^2, was abraded with emery paper to a 2000 metallographic finish, and polished with alumina (α-Al_2O_3 0.05 μm), rinsed in redistilled water and decreased in ethanol. Voltammetric measurements were conducted after 2 h immersion (if not differently reported) in test solution with or without inhibitor. The solution was stirred by a magnetic stirrer.

Atomic force microscopy (AFM): Polished copper samples were immersed in test solutions for different time intervals and afterwards *ex situ* measurements were carried out by NanoScope III (Digital Instrument). Images taken in contact mode were used without further procedures except autoflattening.

SEM/EDX measurements: Samples measured in high vacuum at room temperature were the same as those used in the AFM experiments. The surface morphology and surface composition were measured.

3. Results and discussion

3.1. *Cyclic voltammetry*

The electrochemical behaviour of copper in 3% NaCl solution was studied by cyclic voltammetry. Measurements performed in stirred and quiescent solutions are presented in Figure 1. It can be seen that although the voltammograms present several anodic peaks there is always only one cathodic peak. In addition, the shape of the voltammogram is strongly influenced by solution stirring.

Similar results were obtained by Crousier et al. [12]. They concluded that both anodic peaks represent formation of $CuCl_2^-$. This behaviour can be explained according to the well accepted mechanism of copper dissolution in chloride media (when the $[Cl^-] < 1$ M) [13–17]:

$$Cu + Cl^- \leftrightarrow CuCl + e^- \quad (1)$$

$$CuCl + Cl^- \rightarrow CuCl_2^- \quad (2)$$

According to this mechanism, the first anodic peak (A1) is due to formation of the CuCl precipitate on the electrode surface. This layer is porous and electrochemical reaction can continue through it and a second anodic peak (A2) is observed. The second anodic peak is followed by a current plateau. The intensity of this plateau points to the existence of a poorly protective film. As concluded by Crousier et al. [12], the voltammogram is typical of a mechanism of anodic layer formation in several steps, followed by an equilibrium between dissolution and formation of the layer. During the anodic scan, there is always a balance between CuCl and $CuCl_2^-$ (between film formation and film dissolution). Therefore, solution stirring enhances dissolution of the CuCl film and the anodic current is increased. The cathodic peak (C1) is significantly smaller in the case of stirring, which indicates that the compound to be reduced is moved away from the electrode surface. It can be assumed that cathodic peak represents reduction of $CuCl_2^-$. According to the Pourbaix diagram for copper in chloride solutions [16], Cu_2O can be expected in neutral solutions but Delouis et al. [13, 14] have concluded that it is formed only after longer immersion periods by hydrolysis of CuCl. Reduction charges of Cu_2O layers formed in the 0.5 M sodium chloride solution after different immersion times are reported in the literature [14, 18]. Deslouis et al. found that after immersion for 3 h the charge consumed for Cu_2O reduction was only 8.5 mC cm^{-2}. The charge consumed for the reduction of Cu_2O was even lower in the case of a rotating electrode. Because of increased $CuCl_2^-$ mass transfer towards the bulk solution, the concentration of primary corrosion products near the electrode surface was reduced and an extensive local hydrolysis to Cu_2O [13] was prevented. At shorter immersion periods, the Cu_2O reduction peak was observed near −900 mV, while it shifted towards more negative potentials with a longer immersion time [18]. In our experiments, the amount of Cu_2O that formed at open corrosion potential was low, and was reduced in the cathodic region of the forward scan.

The voltammograms obtained in inhibited and uninhibited quiescent solution are presented in Figure 2. The addition of inhibitor strongly reduced both anodic and cathodic peaks. Two anodic peaks can be observed in the inhibited solution and uninhibited solution. The first peak is much smaller and can be discerned with difficulty. Its potential slightly shifts in the positive direction when compared to the pure NaCl solution. The second anodic peak is observed at 200 mV, while in the uninhibited solution it occurs at 230 mV. As can be

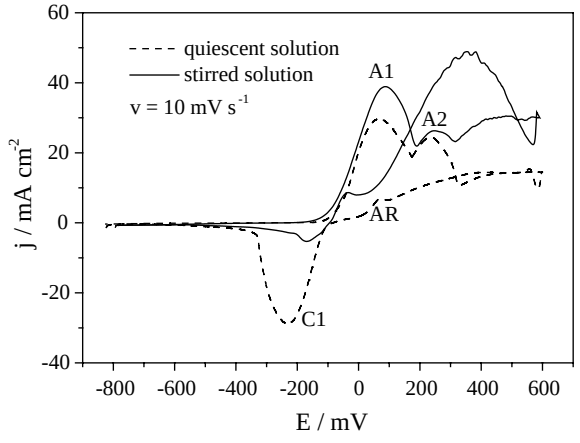

Fig. 1. Cyclic voltammogram for copper in 3% NaCl solution. (A1, A2 – anodic peaks, AR is the anodic reactivation peak while C1 is the cathodic peak).

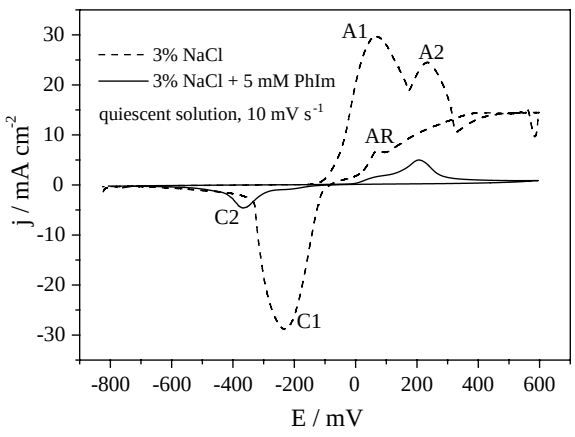

Fig. 2. Cyclic voltammograms of copper in solutions with and without the investigated inhibitor (A1,A2 – anodic peaks, AR–anodic reactivation peak and C1,C2 – cathodic peaks).

seen in Figure 3, these two peaks overlap with increase in scan rate.

In contrast to pure NaCl solution, two cathodic peaks can be observed in the inhibited solution. The potential of the first peak corresponds to the cathodic peak in the uninhibited solution and it shifts in the cathodic direction with increase in scan rate. The second cathodic peak also shifts in the cathodic direction with increase in scan rate, but the current density associated with this peak first increases with scan rate and then decreases at higher scan rates.

Cyclic voltammograms in stirred solution containing inhibitor (Figure 4) are similar to those obtained in the quiescent solution, so that the lower anodic peak currents compared to uninhibited solution are even more pronounced. In the stirred solution, two poorly separated anodic peaks can also be observed. Their potential corresponds to those observed in the quiescent solution. At lower scan rates, the current density of A2 in the stirred solution is lower than in the quiescent solution, while at higher scan rates the reverse behaviour is observed. Two cathodic peaks also appear in the reverse scan. The position of the first peak can be related to the cathodic peak in uninhibited solution. With an increase in scan rate, the potential of the first peak becomes more negative and the peak current increases. The second cathodic peak first moves in the cathodic direction and then, at higher scan rates, in the anodic direction. At all scan rates, cathodic peak currents are lower in the stirred than in the quiescent solution, which is due to the faster dissolution of oxidation products.

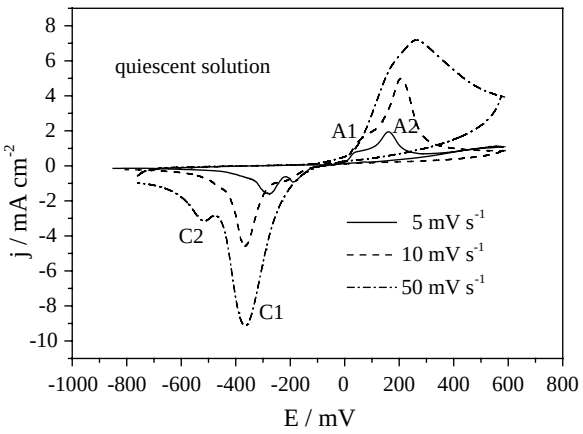

Fig. 3. Cyclic voltammograms of copper in the quiescent 3% NaCl solution containing 5 mM of 1-phenyl-4-methylimidazole (A1,A2 – anodic peaks, AR – anodic reactivation peak and C1, C2 cathodic peaks).

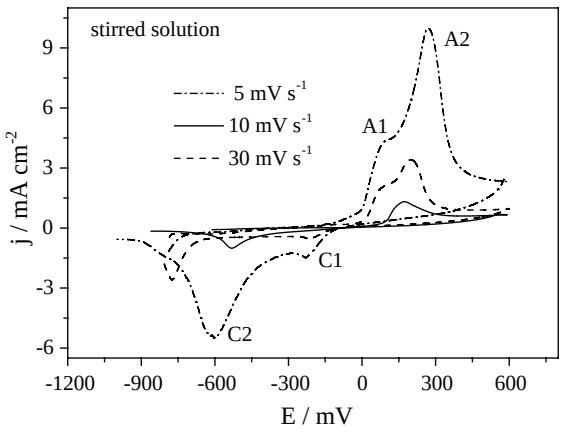

Fig. 4. Cyclic voltammograms of copper in the stirred 3% NaCl solution containing 5 mM of 1-phenyl-4-methylimidazole. (A1,A2 – anodic peaks, AR – anodic reactivation peak and C1, C2 cathodic peaks).

It can be seen in Figures 3 and 4 that shape of the anodic part of the voltammogram is very similar in the stirred and quiescent solutions, while differences in peak height and position is observed in the cathodic part of the voltammogram. The similarity between voltammograms observed in the quiescent and stirred solutions suggests that the corrosion mechanism is the same in both conditions. In the stirred solution, the cathodic peak C1 is smaller than in the quiescent solution. It can therefore be concluded that the soluble and weakly bonded $CuCl_2^-$ is reduced at this point. The second cathodic peak can also be attributed to the reduction of $CuCl_2^-$, but probably of those species which are more strongly bonded to the surface layer.

Table 1. Total charges of anodic (AQ) and cathodic (CQ) processes

Solution	Measurement	Scan rate /mV s^{-1}	AQ /mC cm^{-2}	CQ /mC cm^{-2}
Stirred	*3% NaCl*	*10*	*3932*	*−104*
	3% NaCl + 5 mM 1-phenyl-4-methylimidazole	5	127	−66
		10	116	−47
		20	96	−49
		50	93	−46
Quiescent	*3% NaCl*	*10*	*1905*	*−469*
	3% NaCl + 5 mM 1-phenyl-4-methylimidazole	5	196	−68
		10	132	−74
		20	113	−59
		50	78	−40

The total charges of the anodic (QA) and cathodic (QC) processes are determined by the integration of the anodic and cathodic current peaks (Table 1). In the uninhibited solution, the total anodic charge is much higher than the cathodic charge, which is due to $CuCl_2^-$ removal from the electrode surface, especially in the case of the stirred system. In inhibited solutions (both stirred and quiescent) the ratio between the total anodic and cathodic charges is about 2 and does not change with scan rate. This indicates that a half of the CuCl produced during the anodic scan has been removed from the electrode surface due to dissolution and diffusion into the bulk solution. This ratio may be a measure of $CuCl/CuCl_2^-$ binding with the surface layer, but also of the porosity of this layer.

At lower scan rates, the total charges measured in the stirred solution are lower than in the quiescent solution, while at higher scan rates the reverse behavior is observed. This fact may be related to the influence of stirring on mass transport processes (the transport of Cl^- ions to the electrode surface and the transport of $CuCl_2^-$ from the electrode). The Cl^- content in the solution is much higher when compared to the inhibitor content, so that at lower scan rates the stirring enhances inhibitor transport to the electrode surface, while the concentration of Cl^- near the electrode surface is not highly influenced by stirring. At higher scan rates, the stirring is not efficient enough to supply a sufficient amount of inhibitor, while the transport rate of Cl^- and $CuCl_2^-$ is sufficiently enhanced.

Voltammetric measurements were performed after different immersion times (Figure 5) in order to further characterize the protective properties of the surface layer. After initial 30 min of immersion, the protection of copper against corrosion by the inhibitor layer is quite poor, and anodic peak currents and charges are only slightly lower than in the case of the uninhibited solution. After one-hour immersion, the inhibitor layer properties are much better and the voltammogram already has the shape previously observed for the inhibited system. Two cathodic peaks are observed, the first at the position where $CuCl_2^-$ reduction occurs in the pure NaCl solution, and the second at a more negative potential. The anodic peak currents and total anodic charges decrease with increase in immersion time, which points to improvement of the protecting layer. The first cathodic peak decreases with immersion time so that only the reduction peak C2 can be observed after six-hour immersion. This second peak probably presents reduction of $CuCl_2^-$, just like the first cathodic peak. However, its reduction potential is shifted to more negative values due to the blocking effect of the surface layer. It is very likely that this peak does not represent reduction of Cu_2O because the reduction of this compound was observed in the cathodic region of the forward scan at much lower potentials, as mentioned previously.

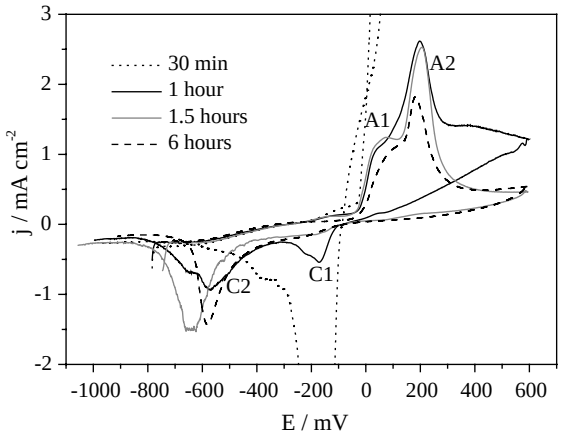

Fig. 5. Influence of immersion time on inhibitor layer properties, measured in the stirred solution. Scan rate 5 mV s^{-1}. (A1,A2 – anodic peaks, AR – anodic reactivation peak and C1, C2 cathodic peaks).

For shorter immersion periods, the total anodic charge is much higher than the total cathodic charge, which is an indication of significant dissolution of the CuCl film due to defects in the inhibitor layer and its permeability. This ratio decreases with immersion time and reaches, after 1.5 h, a value of about 2, and does not change further with additional increase in immersion time. It was also observed that the corrosion potential shifts in the positive direction for about 100 mV after 1 h of immersion. All these observations imply that the protective properties of the surface layer improve with aging.

3.2. *AFM measurements*

Topographical changes of the copper surface were qualitatively characterized by AFM. The images were taken after immersion for 2 h. In uninhibited 3% NaCl solution, deep pits ($\Delta Z = 223$ nm) were observed on the copper surface (Figure 6(a)). More detailed AFM studies of time dependant morphological changes in neutral chloride solution can be found in the literature [19]. In the very early stages of immersion a net of polymer-like depositions appeared on the surface of the copper sample immersed in the inhibited solution. The surface after 30 min of immersion in the inhibited solution is shown in Figure 6(b). The coverage of the metal surface increased significantly with time. After 2 h, the entire metal surface was covered with a rough layer of precipitate forming a barrier to aggressive ions (Figure 6(c)).

3.3. *SEM/EDX measurements*

SEM/EDX analyses were conducted in order to characterize the protective layer that formed on the copper surface. SEM images in the uninhibited and inhibited solutions are presented in Figure 7(a) and 7(b), respectively. After 30 min of immersion in the inhibited solution, the copper surface was partly covered with a layer containing not only the carbon, but also the

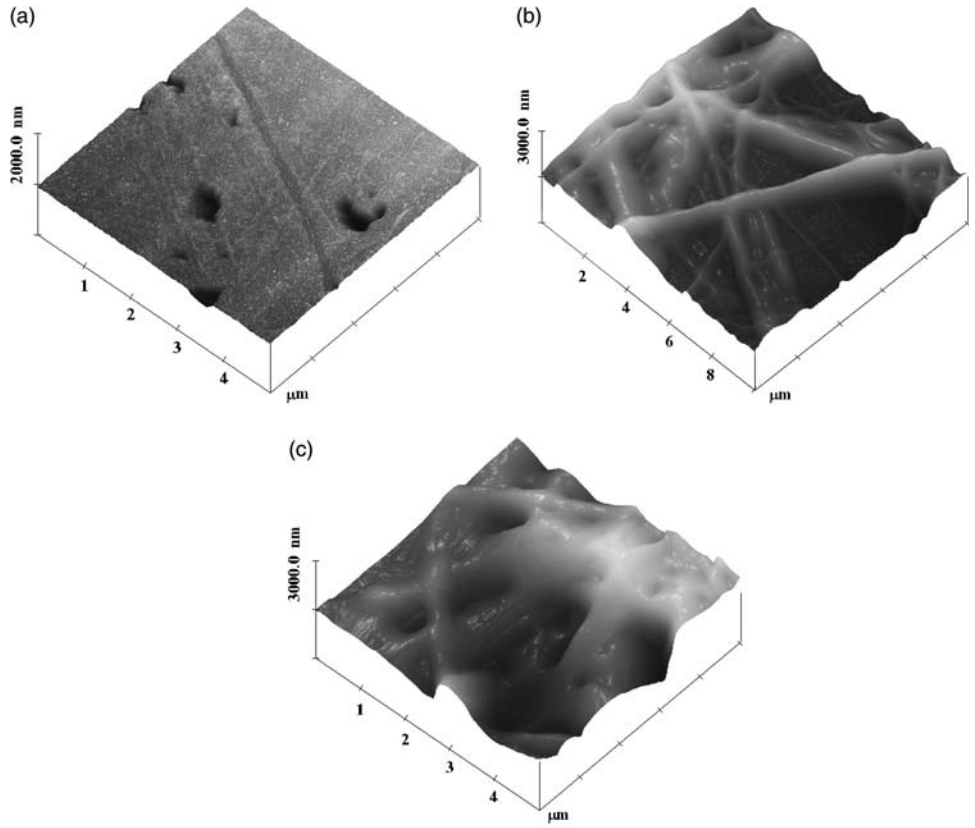

Fig. 6. AFM images of copper in 3% NaCl solution after two-hour immersion (a); in 3% NaCl solution with 5 mM of 1-phenyl-4-methylimidazole after 30 min of immersion (b); two-hour immersion (c).

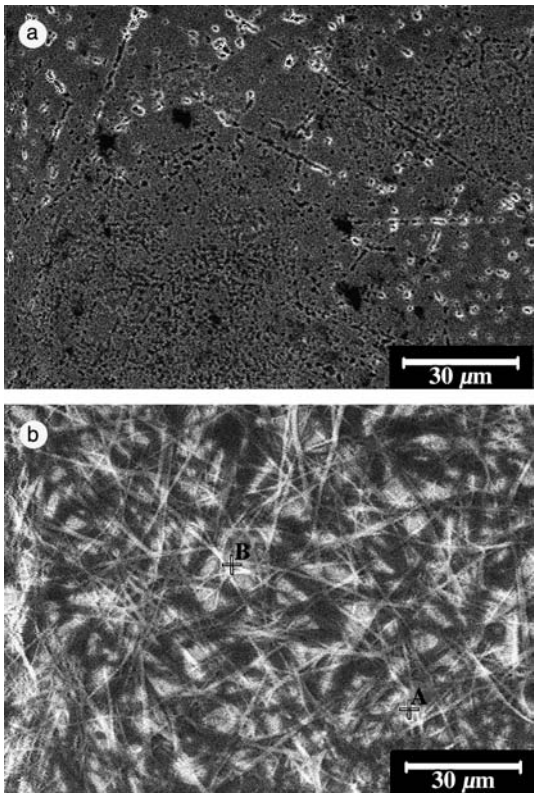

Fig. 7. SEM images of copper in 3% NaCl solution after two-hour immersion (a); in inhibited solution after 30 min immersion (b).

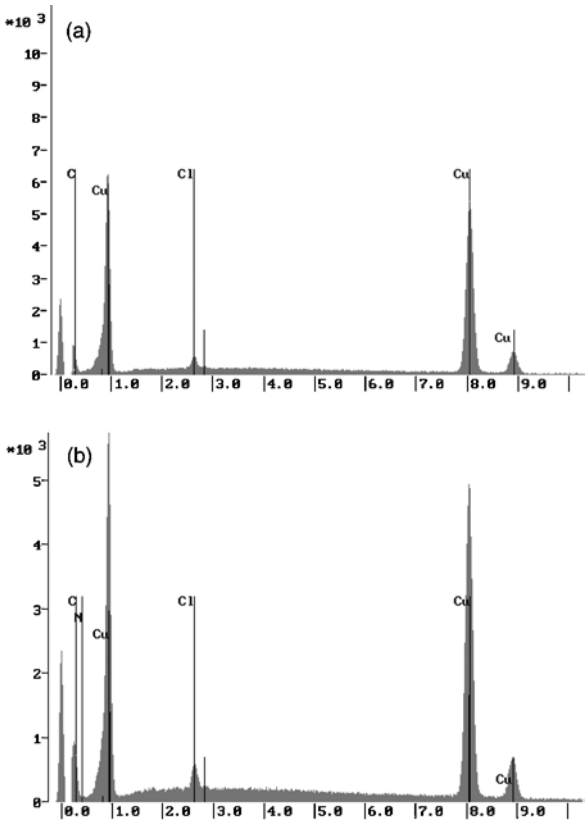

Fig. 8. EDX analysis of the copper surface after 30 min of immersion in the inhibited solution: average surface composition (a) and composition at point B (b).

chloride. The ratio of C to Cl varies between 2 and 4. In addition to the analysis of the complete surface (Figure 8(a)), EDX analysis was performed at point B where the interface layer was supposed to be thick (Figure 8(b)). It can be concluded from this analysis that chlorides are incorporated in the inhibitor layer either as precipitate or, more likely, as a part of the protective layer.

4. Conclusions

The corrosion of copper in neutral chloride solutions is strongly reduced in the presence of 1-phenyl-4-methyl-imidazole. This compound forms a thick protective layer on the copper surface. The layer does not influence the corrosion mechanism, but mostly acts by blocking the electrode surface. The protection offered by this layer improves with immersion time. From SEM/EDX measurements, it can be concluded that the layer consists of the inhibitor and corrosion products: the exact structure will be the subject of further investigations.

Acknowledgements

The financial support from the Ministry of Science and Technology of the Republic of Croatia under Project 0125012 is gratefully acknowledged.

References

1. Y.I. Kuznetsov, 'Organic Inhibitors for Corrosion of Metals' (Plenum, New York, 1996).
2. M. Fleischmann, I.R. Hill, G. Mengoli, M.M. Musiani and J. Akhavan, *Electrochim. Acta* **30** (1985) 879.
3. A. Dafali, B. Hammouti, A. Aouniti, R. Mokhlisse, S. Kertit and K. Elkacem, *Ann. Chim. Sci. Mat.* **25** (2000) 437.
4. G. Xue, J. Ding, P. Wu and G. Ji, J. *Electroanal. Chem.* **270** (1989) 163.
5. W.J. Lee, *Mater. Sci. Eng. A* **348** (2003) 217.
6. C. McCrory-Joy and J.M. Rosamilia, *J. Electroanal. Chem.* **136** (1982) 105.
7. B. Trachili, M. Keddam, H. Takenouti and A. Srhiri, *Prog. Org. Coat.* **44** (2002) 17.
8. E. Stupnišek-Lisac, V. Cinotti and D. Reichenbach, *J. Appl. Electrochem.* **29** (1999)117.
9. E. Stupnišek-Lisac, A. Gazivoda and M. Madžarac, *Electrochim. Acta* **47** (2002) 4189.
10. R. Gašparac, C.R. Martin and E. Stupnišek-Lisac, *J. Electrochem. Soc.* **147** (2000) 548.
11. H. Otmačić and E. Stupnišek-Lisac, *Electrochim. Acta* **48** (2003) 985.
12. J. Crousier, L. Paradessus and J.P. Crousier, *Electrochim. Acta* **33** (1988) 1039.
13. C. Deslouis, B. Tribollet, G. Mengoli and M.M. Musiani, *J. Appl. Electrochem.* **18** (1988) 374.
14. C. Deslouis, B. Tribollet, G. Mengoli and M.M. Musiani, *J. Appl. Electrochem.* **18** (1988) 384.
15. H.P. Lee and K. Nobe, *J. Electrochem. Soc.* **133** (1986) 2035.
16. D. Tromans and R. Sun, *J. Electrochem. Soc.* **138** (1991) 3235.
17. D. Tromans and J.C. Silva, *Corrosion* **53** (1997) 16.
18. B. Millet, C. Fiaud, C. Hinnen and E.M.M. Sutter, *Corros. Sci.* **37** (1995) 1903.
19. A. Shaban, E. Kálmán, J. Telegdi and G. Pálinkás, Gy. Dóra, *Appl. Phys. A* **66** (1998) S545.